Early Ordovician orogenic event in Galicia (NW Spain): evidence from U–Pb ages in the uppermost unit of the Ordenes Complex

J. Abati [a,*], G.R. Dunning [b], R. Arenas [a], F. Díaz García [c], P. González Cuadra [d], J.R. Martínez Catalán [d], P. Andonaegui [a]

[a] *Departamento de Petrología y Geoquímica, Universidad Complutense, 28040 Madrid, Spain*
[b] *Department of Earth Sciences, Memorial University, St. John's, NF A1B 3X5, Canada*
[c] *Departamento de Geología, Universidad de Oviedo, 33005 Oviedo, Spain*
[d] *Departamento de Geología, Universidad de Salamanca, 37008 Salamanca, Spain*

Abstract

New U–Pb data (zircon, monazite and rutile) obtained from rocks of the uppermost allochthon in the Variscan belt of NW Spain indicate that the hangingwall to the suture includes an allochthonous unit with a pre-Variscan tectonothermal evolution. This evolution is characterised by an Early Ordovician (498–500 Ma) bimodal magmatism followed almost immediately (493–498 Ma) by a Barrovian style metamorphism up to the granulite facies. The metamorphism subsequent to the igneous intrusions requires convergence and crustal thickening in order to generate the Barrovian facies pattern shown by the lithologies of the uppermost allochthon. The almost coeval magmatism and metamorphism, and the chemistry of the metabasites suggest an accretionary complex, probably related to a volcanic arc, as the most probable setting for the origin of the uppermost unit. The implications of the existence of Early Ordovician convergent plate boundaries are discussed in the context of Gondwana–Laurentia–Avalon interactions.

Keywords: U/Pb; geochronology; Ordovician; thermal metamorphism; Hercynian orogeny; Galicia Spain

1. Introduction

The geology of the Northwest Iberian Massif represents a complete transition from the external to the axial zones of the Variscan belt. Five allochthonous complexes, located in Galicia (Spain) and Trás-os-Montes (Portugal), occupy the uppermost structural position in the axial zone. They consist of a pile of units stacked at the onset of the Variscan deformation, and include a suture zone marked by several slices of oceanic lithosphere [1,2]. From bottom to top, the allochthonous units are grouped into basal, ophiolitic and upper units (Fig. 1). During the main Variscan deformation, these units were thrust over the Iberian autochthon [1], which represents the larger part of the Iberian Massif.

The occurrence of a suture points to a collisional process and there is general agreement that one of the colliding elements was the continental margin of Gondwana, represented by the units in the footwall to the suture: the Iberian autochthon and the allochthonous basal units [2–4]. The origin and significance of the units in the hangingwall to the

* Corresponding author. Tel.: +34-91-394-4898; Fax: +34-91-544-2535; E-mail: abati@eucmax.sim.ucm.es

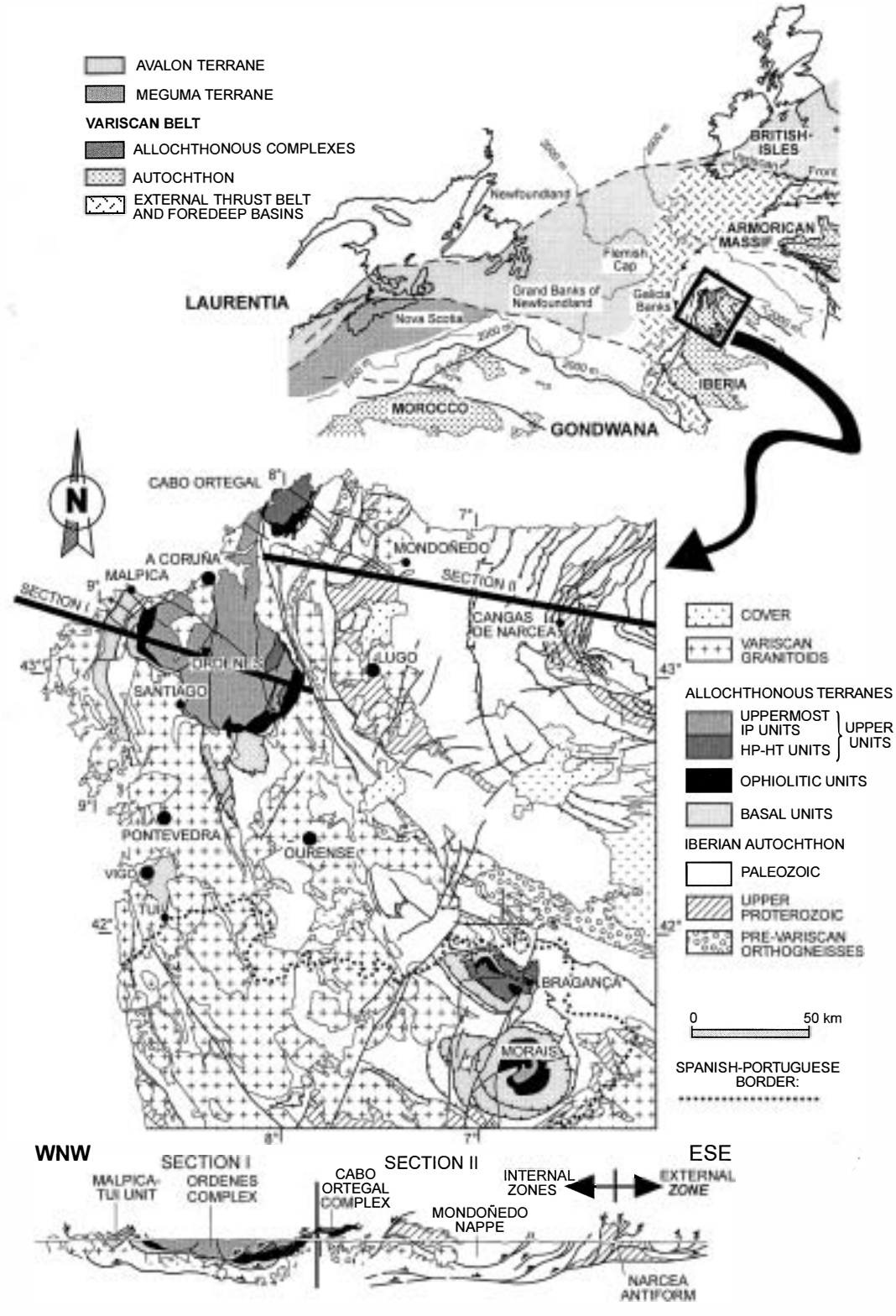
AVALON TERRANE
MEGUMA TERRANE
VARISCAN BELT
ALLOCHTHONOUS COMPLEXES
AUTOCHTHON
EXTERNAL THRUST BELT AND FOREDEEP BASINS
BRITISH-ISLES
Newfoundland
ARMORICAN MASSIF
Flemish Cap
LAURENTIA
Grand Banks of Newfoundland
Galicia Banks
Nova Scotia
IBERIA
MOROCCO
GONDWANA
N
CABO ORTEGAL
A CORUÑA
MALPICA
MONDOÑEDO
SECTION I
SECTION II
CANGAS DE NARCEA
LUGO
SANTIAGO
PONTEVEDRA
OURENSE
VIGO
TUI
BRAGANÇA
MORAIS
43°
42°
9°
8°
7°
COVER
VARISCAN GRANITOIDS
ALLOCHTHONOUS TERRANES
UPPERMOST IP UNITS
HP-HT UNITS
UPPER UNITS
OPHIOLITIC UNITS
BASAL UNITS
IBERIAN AUTOCHTHON
PALEOZOIC
UPPER PROTEROZOIC
PRE-VARISCAN ORTHOGNEISSES
0
50 km
SPANISH-PORTUGUESE BORDER:
WNW
SECTION I
SECTION II
ESE
MALPICA-TUI UNIT
ORDENES COMPLEX
CABO ORTEGAL COMPLEX
INTERNAL ZONES
EXTERNAL ZONE
MONDOÑEDO NAPPE
NARCEA ANTIFORM

suture, representing the other colliding element, is more problematic, and has been the source of a prolonged controversy due to the lack of unambiguous dating of deformation and metamorphism. As can be seen in Fig. 1, two different types of units can be distinguished above the ophiolites: the lower high-pressure and high-temperature (HP–HT) units and an intermediate-pressure (IP) uppermost unit. Isotopic dating has been carried out previously in both units, and results are interpreted as either protolith or metamorphic ages. However, data relevant to the timing of metamorphism have been reported only for the HP–HT units, and the most recent results have been interpreted as indicative of an early Variscan age for the initial, high-pressure event [5–7].

The aim of this study is to date accurately the bimodal magmatism and the metamorphism of the uppermost unit of the Ordenes Complex, in order to constrain the origin and tectonothermal evolution of the problematic colliding element, presently above the suture. The magmatism has been dated by the U–Pb method, analysing magmatic zircon populations from gabbros and orthogneisses. To determine the timing of high-grade metamorphism, U–Pb analyses have been carried out on monazite included in biotite belonging to the regional tectonic foliation of paragneisses of the sillimanite zone. Due to the elevated closing temperature of monazite, above 700–725°C [8–10], it is very likely that the mineral ages provide the age of the metamorphic thermal peak.

2. Geological setting

The Ordenes Complex is the largest of the allochthonous complexes preserved as mega-klippen in the axial part of the Iberian Massif. It consists of a stack of thrust sheets, overprinted by extensional detachments, upright folds and faults. The complex is underlain and surrounded by relatively autochthonous sequences.

The autochthon, together with other comparable terranes of southern Europe, formed part of the continental margin of Gondwana during the Neoproterozoic and Paleozoic. This margin registered the Cadomian (Pan-African) orogeny, as well as Cambrian–Ordovician continental rifting processes, which resulted in the pulling away of the Avalon microcontinent (or microcontinents) from the Gondwana mainland and the opening of the Rheic oceanic domain [11,12].

The allochthonous tectonostratigraphic units, which also occur in the other Iberian allochthonous complexes, can be classified according to their lithological associations and tectonothermal evolution, and also according to their relative position [2,13,14]. What follows is a brief description of these units.

2.1. Basal units

The basal units consist of schists, paragneisses, and alternating igneous felsic and mafic rocks. Granitic and peralkaline orthogneisses have yielded U–Pb and Rb–Sr ages of 480–460 Ma [15,16]. The magmatism is interpreted to reflect an Ordovician rifting episode [17]. Since there are no ophiolites separating them from the underlying parautochthon, the basal units are considered part of the continental margin of Gondwana formed after the opening of an ocean, subsequent to the Ordovician rifting.

However, the basal units are considered allochthonous because there is a pressure gap in the metamorphic evolution between them and the parautochthon. The basal units underwent an initial subduction-related HP metamorphic event, which reached 14–16 kbar and 650–700°C [14,18]. The final stages of subduction have probably occurred 374 m.y. ago, the age of post-eclogitic white micas [15]. The polarity of subduction was roughly to the west in present coordinates [2].

2.2. Ophiolitic units

The ophiolitic units appear repeated in several thrust sheets and include metapelites and cherts, basalts, pillow breccias and hyaloclastites, diabases, metagabbros, plagiogranites, amphibolites and ultramafic rocks. In the Ordenes Complex, the upper

Fig. 1. Geological map and cross-section of the NW Iberian Massif, showing the allochthonous complexes and their units. The location of the mapped area is shown in the upper part of the figure, in a reconstruction of Pangea based on Lefort [49].

thrust sheet represents the basal parts of an ophiolitic sequence, characterised by the abundance of pegmatitic gabbros. A protolith age of 395 ± 2 has been obtained for a gabbro differentiate in this unit [19]. Other ophiolitic units seem to represent the upper parts of the oceanic lithosphere, because of the abundance of pelitic sediments and greenstones partially derived from basalts.

The ophiolites show a wide variety of metamorphic conditions, ranging from intermediate-pressure granulite facies to amphibolite and greenschist facies. A high-pressure metamorphic gradient has been identified in some of the thrust sheets. The ophiolitic nappes show eastward vergence, and were stacked during the closure of a previously opened ocean. The coeval amphibolite-facies foliation in the medium-grade units was formed 390–380 m.y. ago [20], closely following oceanic crust generation.

2.3. *Upper units*

The upper units structurally overlie the ophiolites and can be subdivided into HP–HT units, below, and an IP unit occupying the uppermost structural position.

2.3.1. *High-pressure and high-temperature units*

The HP–HT units consist of paragneisses, metabasites, and ultramafic rocks. The metabasites are garnet–clinopyroxene granulites and eclogites, retrograded to the amphibolite facies. The REE patterns of eclogites and some of the mafic units in the Cabo Ortegal Complex are characteristic of the oceanic crust [21]. However, the abundance of sediments points to a different origin for many of the units. Gabbros occur in several stages of transformation, from virtually undeformed and scarcely affected by the metamorphism, to coronitic metagabbros and HP granulites. In the less deformed gabbros, subophitic and diabase textures have been preserved, indicating an emplacement at relatively shallow levels. The chemical characteristics of the gabbros are comparable to modern continental tholeiites, and compatible with a continental rift provenance [22,23].

The peak metamorphic conditions recorded by the HP–HT units are variable, reaching at least 18 kbar, and 700–850°C [21]. Several early Paleozoic U–Pb ages, between 490 and 480 Ma [21], were currently interpreted as dating the HP–HT metamorphism, but Schäfer et al. [5] consider these the ages of the mafic protoliths. Schäfer et al. [5], Santos Zalduegui et al. [6] and Ordóñez Casado et al. [7] have obtained U–Pb ages on zircon, monazite and titanite indicating a metamorphic event between 405 and 390 m.y. ago. According to the authors, these ages correspond to the HP–HT event, which was followed by a subsequent retrograde amphibolite-facies metamorphism at 390–380 Ma [20,24].

2.3.2. *Uppermost unit with intermediate-pressure metamorphism*

The unit consists of a thick sequence of terrigenous metasediments, and large bodies of augengneisses, amphibolites and gabbros. The metasedimentary sequence is known as the Ordenes Series. In the epizonal upper part, the metasediments are a succession, 2000–3000 m thick, of pelites and greywackes [25]. Generalised graded bedding and other abundant sedimentary structures indicate a flyschoid character. The augengneisses show intrusive relationships with the metasediments, and have yielded ages of 496–460 Ma (U–Pb on zircons: [26,27]). The gabbros are also intrusive, and deformed diabase dikes are common in the augengneisses and metasediments.

The metamorphism ranges from high-grade at the basal part of the unit, to epizonal in the upper part. Several metamorphic zones have been mapped, and their limits are commonly extensional detachments, a feature also present in other allochthonous units, that indicates a strong thinning of the original nappe pile [2,13,14,18].

The deepest part of the uppermost IP unit is occupied by a large, rounded metagabbroic body, the Monte Castelo Gabbro (MCG), outcropping in the western part of the Ordenes Complex (Fig. 2). This is a massive two-pyroxene gabbro, fine- to medium-grained, with textures variable from granular to intergranular and ophitic. The igneous mineral assemblage consists of clinopyroxene, orthopyroxene, plagioclase, occasional olivine, biotite and hornblende, and ilmenite, titanite, and zircon as accessory minerals. The presence of olivine and the common ophitic textures point to a relatively shallow emplacement. The MCG is tholeiitic in character. A detailed geochemistry study is in progress, and

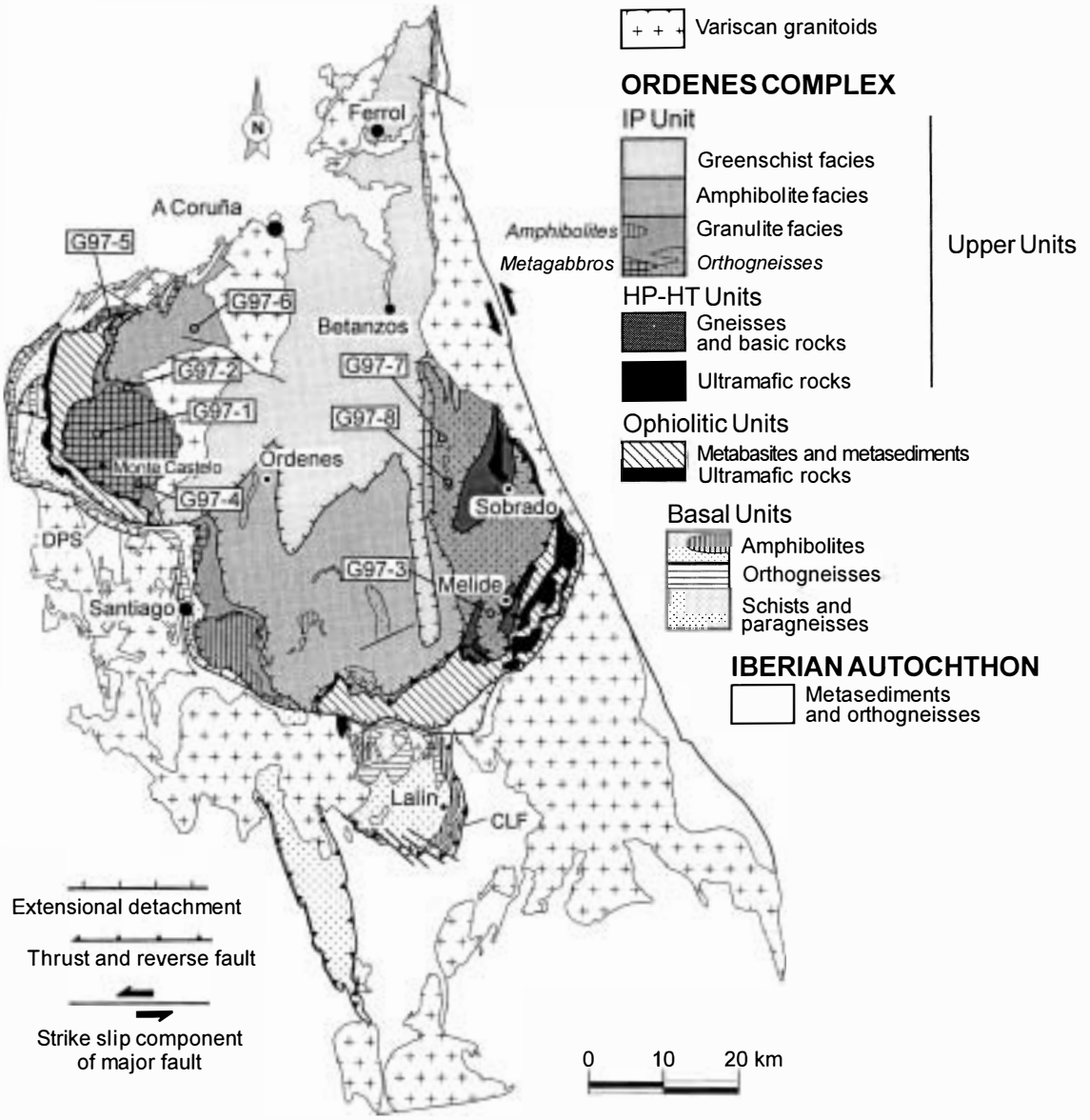

Fig. 2. Geological map of the Ordenes Complex. Outlined are the different units of the complex, the metamorphic zones of the uppermost unit, and the location of the samples collected for U–Pb geochronology.

includes major and trace elements, and REE data. When plotted in multi-element normalised diagrams for comparison with basaltic compositions and tectonic discrimination diagrams, the analyses usually fall in fields related to volcanic arcs.

Near its bottom, the gabbro is cross-cut by granulite-facies prograde shear zones, which produced a complete recrystallisation of the igneous paragenesis and display a new metamorphic assemblage consisting of garnet, orthopyroxene, biotite, plagioclase, quartz, ilmenite, and rutile, arranged in a granoblastic to grano-lepidoblastic texture.

Scarce metapelitic enclaves in the MCG show also a granulite-facies mineral assemblage, compatible with that of the host rock, that includes garnet, orthopyroxene, biotite, plagioclase, K-feldspar, quartz,

sillimanite, ilmenite, and rutile. At the outcrop scale or in hand specimen, a high-grade foliation is evident in these granulites, which excludes the possibility of an origin by contact metamorphism. The less retrogressed samples contain rounded, coarse garnet (up to 1 cm) in a granoblastic polygonal matrix formed by plagioclase, quartz, K-feldspar, and subeuhedral elongated orthopyroxene and reddish biotite. The peak mineral associations from the gabbro and the metasedimentary enclaves suggest temperatures above 750–800°C and intermediate pressures.

Overlying and surrounding the MCG, a thick pile of monotonous plagioclase-rich paragneisses occurs. In some places, the contact between the gabbro and the metasediments of the Ordenes Series contains narrow granitic bands (50–100 m thick), probably generated by partial melting of the latter. In some outcrops, the granites appear deformed and show a plano-linear fabric and abundant enclaves (restites) of paragneisses from the surrounding metasediments. These fine- to medium-grained granitoids contain quartz, plagioclase, biotite, muscovite, clinozoisite and small amounts of ilmenite, chlorite, and zircon. To the north of the MCG, the paragneisses contain the peak mineral assemblage garnet, biotite, muscovite, plagioclase, quartz, sillimanite, and ilmenite, belonging to the first sillimanite zone. Generally, they are strongly retrogressed to the greenschist facies, showing the breakdown of garnet and biotite to chlorite and the sillimanite being limited to needles included in muscovite.

In the eastern part of the complex, the metamorphic conditions of the Ordenes Series are slightly higher, reaching the sillimanite–K-feldspar zone and showing abundant evidence of partial melting. A large outcrop of granitic augengneiss (the Corredoiras Orthogneiss) is located at the base of the unit, in a position equivalent to that of the MCG, and is separated from the underlying HP–HT units by a ductile shear zone, the Corredoiras Detachment [2] (Fig. 2). The orthogneiss also shows evidence of the high-grade metamorphic event, such as garnet coronas around biotite and recrystallised muscovite-free domains composed of garnet, biotite, plagioclase, K-feldspar, quartz, sillimanite, ilmenite, and rutile. The orthogneiss includes large bodies of migmatitic paragneisses with high-grade mineral assemblages with garnet, biotite, K-feldspar, plagioclase, quartz, sillimanite, and minor cordierite. The relationships between augengneisses and migmatites at the outcrop scale, suggest that the high-grade metasediments were initially large xenoliths in the granitic body (probably originating in a crustal region subjected to partial melting), and were subsequently deformed and metamorphosed together with the host granitic rocks.

The central part of the Ordenes Complex is essentially a pelitic and semipelitic sequence of rocks in which Barrovian kyanite, staurolite, and garnet zones can be recognised. In the upper part of the sequence, separated from the central part by an extensional detachment (Fig. 2), the metamorphism is of low grade, the igneous rocks are scarce, and the dominant lithologies are schists in the garnet and biotite zones, and slates, phyllites and metagreywackes in the chlorite zone.

3. U–Pb geochronology

3.1. Selection of samples

Eight samples were selected for U–Pb geochronology in order to establish the age of magmatism and metamorphism in the uppermost unit of the Ordenes Complex. Five of the samples are high-grade paragneisses and the other three are meta-igneous rocks. Sample localities are shown in Fig. 2. Felsic and mafic igneous rock types were selected to confirm the contemporaneity of the bimodal magmatism, suggested by the field relationships. The metasediments were selected from different high-grade metamorphic conditions (from sillimanite to orthopyroxene zones) to investigate possible age differences relevant to their tectonothermal evolution. For that purpose, zircon from the igneous rocks and monazite fractions from the metasedimentary rock samples were recovered; in addition, rutile was separated from G97-4 in order to obtain cooling ages in an attempt to constrain the timing of retrogression.

G97-1 is a gabbro from the central part of the MCG, sampled in a zone with abundant pegmatoids, where quartz was visible in the field, to ensure the presence of enough zircon. The texture is intergranular and scarce olivine is present in the non-pegmatitic zones.

G97-2 is a granitoid rock located in the contact

between the MCG and the Ordenes Series, sampled in a zone free of enclaves and slightly deformed. The rock is fine- to medium-grained, and has abundant mica-fishes of biotite, recrystallised quartz mosaics and porphyroclasts of plagioclase and clinozoisite. Accessory minerals are ilmenite, generally surrounded by titanite, and zircons included in biotite with a mean size of 0.2 mm.

G97-3 is an augengneiss from the Corredoiras Massif. This coarse- to very coarse-grained metagranite shows large K-feldspar megacrysts (up to 7 cm), surrounded by a moderately recrystallised matrix with plagioclase, quartz, biotite, garnet, ilmenite and titanite.

G97-4 is a metapelitic granulite-facies xenolith collected in the southern part of the MCG. The paragneiss exhibits a well-preserved high-temperature mineral assemblage with garnet, orthopyroxene, biotite, sillimanite, rutile, ilmenite, K-feldspar, plagioclase and quartz. Light yellow monazite with pleochroic halos can easily be identified as inclusions in biotite.

G97-5 and G97-6 are semi-pelitic paragneisses of the sillimanite zone from the western part of the uppermost unit. They are fine- to medium-grained and show a gneissic foliation defined by domains rich in biotite, muscovite and scarce sillimanite, alternating with quartz–plagioclase domains. Garnet and ilmenite are present in both domains, and numerous zircon and monazite grains can be seen included in the biotite defining the fabric.

G97-7 and G97-8 are fine- to medium-grained migmatites from the eastern part of the uppermost unit, outcropping as regional scale mega-enclaves in the Corredoiras Orthogneiss. The gneisses are granolepidoblastic and contain the peak mineral assemblage garnet, biotite, plagioclase, K-feldspar and sillimanite. Cordierite is also present as a secondary phase.

3.2. Analytical techniques

All the steps of U–Pb method were carried out in the Department of Earth Sciences, Memorial University of Newfoundland (Canada). The laboratory procedures resemble, in general terms, those described by Dubé et al. [28].

The samples were powdered and mineral fractions were obtained by density separation on a Wilfley table and heavy liquids (Methylene iodide), and by magnetic separation using a Frantz isodynamic separator. After sieving with a 70 mesh sieve, final mineral fractions for analyses were hand-picked under a binocular microscope selecting the crystals according to criteria of morphology, size, colour and clarity. The abrasion technique after Krogh [29] was used to remove the outer surfaces of the minerals to minimise Pb loss, except in the smallest or delicate fractions which are indicated in Table 1. Then, the minerals were cleaned in an ultrasonic bath with low Pb blank 4 N HNO_3, doubly distilled H_2O, and distilled acetone, and subsequently weighed in a microbalance. The mineral fractions were mixed with $^{205}Pb/^{235}U$ isotopic tracer. Zircon and rutile fractions were dissolved for 5 days at 210°C in 8 N HNO_3 and concentrated HF using Teflon bombs sealed by stainless steel jackets. Monazite fractions were digested in 6 N HCl using Savillex Teflon vials placed on a hot plate at 150°C.

The U and Pb were separated by ion exchange chemistry in columns with DOWEX AG1-X8 resin in chloride form, following a modified method of Krogh [30] for zircon, and HBr chemistry after Manhès et al. [31] for monazite and rutile. Purified Pb and U were loaded together on single Re filaments with silica gel and H_3PO_4. Isotope ratios have been measured using a Finnigan-MAT 262 multicollector thermal ionisation mass spectrometer in static mode, with faraday cups calibrated against NBS 981 and with ^{204}Pb measured in the secondary electron multiplier (SEM) in ion counting mode. The only exceptions were the rutile fractions, because their low U and radiogenic Pb contents made it necessary to measure all the Pb ratios by peak jumping using the SEM-ion counter.

Uncertainties on ages and isotope ratios are reported at 2σ, considering the propagation of errors from the measurement by mass spectrometry, the isotope fractionation, the Pb and U blanks (2–12 pg Pb, 1 pg U), and the uncertainty on the isotope composition of initial common Pb, according to the model of Stacey and Kramers [32]. The above calculation of uncertainties was made using an unpublished program of the Royal Ontario Museum, Canada, and the uncertainty on the ages are reported at 95% confidence level.

Table 1
U/Pb data

Fraction	Weight (mg)	Model Th/U	Concentration		Measured		Corrected atomic ratios [a]				Apparent ages (Ma)		
			U (ppm)	Pb rad. (ppm)	Pb com. (pg)	$^{206}Pb/^{204}Pb$	$^{208}Pb/^{206}Pb$	$^{206}Pb/^{238}U$	$^{207}Pb/^{235}U$	$^{207}Pb/^{206}Pb$	$^{206}Pb/^{238}U$	$^{207}Pb/^{235}U$	$^{207}Pb/^{206}Pb$
G97-1 (Monte Castelo Gabbro)													
Z1 fragmented prisms	0.529	0.513	220	18.6	9	64327	0.1644	0.08046 ± 28	0.6342 ± 24	0.05716 ± 6	499	499	498
Z2 fragmented prisms	0.130	0.495	227	19.1	22	6768	0.1591	0.08023 ± 30	0.6332 ± 22	0.05724 ± 10	497	498	501
Z3 fragmented prisms	0.130	0.547	222	18.9	20	7144	0.1756	0.08028 ± 26	0.6336 ± 22	0.05724 ± 8	498	498	501
G97-2 (granitoid)													
M1 small grains	0.085	35.887	1188	1023.5	37	13673	11.4881	0.07921 ± 28	0.6206 ± 22	0.05683 ± 10	491	490	485
M2 coarse grains	0.081	45.455	904	975.2	25	15028	14.4444	0.08028 ± 30	0.6301 ± 24	0.05692 ± 8	498	496	489
Z1 prismatic, clear, small grains	0.054	0.357	211	17.1	18	3249	0.1146	0.08038 ± 34	0.6349 ± 26	0.05729 ± 14	498	499	503
Z2 prismatic, clear, coarse grains	0.060	0.389	228	18.6	20	3406	0.1249	0.08032 ± 30	0.6346 ± 24	0.05730 ± 12	498	499	503
G97-3 (Corredoiras Orthogneiss)													
Z1 clear, euhedral, small	0.211		205	16.3	17	12500	0.0957	0.07982 ± 24	0.6297 ± 20	0.05721 ± 6	495	496	500
G97-4 (Metapelitic enclave in MCG)													
M1 pale yellow, euhedral	0.099	36.824	1127	1012.0	64	8851	11.831	0.08039 ± 28	0.6325 ± 24	0.05707 ± 8	498	498	494
M2 pale yellow, euhedral	0.108	42.403	1034	1039.3	66	8573	13.381	0.08035 ± 34	0.6319 ± 28	0.05704 ± 8	498	497	493
R1 red	0.130	1.150	5	0.4	43	75	0.3702	0.06256 ± 34	0.4825 ± 206	0.05594 ± 222	391	400	450
R2 reddish brown	0.220	0.706	4	0.3	50	82	0.2282	0.06101 ± 30	0.4658 ± 92	0.05538 ± 100	382	388	427
G97-5 (Ordenes Series paragneiss)													
M1 small grains, turbid	0.061	5.463	7074	1363.7	70	30979	1.733	0.07994 ± 32	0.6297 ± 26	0.05714 ± 4	496	496	497
M2 small grains, turbid	0.018	4.783	6677	1199.3	69	8710	1.541	0.07999 ± 46	0.6306 ± 38	0.05718 ± 6	496	496	498
G97-6 (Ordenes Series paragneiss)													
M1 rounded, clear, yellow, not abraded	0.046	3.385	8446	1242.1	31	62253	1.087	0.07943 ± 28	0.6247 ± 24	0.05704 ± 4	493	493	493
M2 8 grains, not abraded	0.008	4.568	6497	1108.5	21	12459	1.454	0.07850 ± 24	0.6168 ± 21	0.05699 ± 6	487	488	491
G97-7 (Ordenes Series migmatite)													
M1 small grains, turbid, not abraded	0.020	6.958	4650	1054.9	32	14306	2.242	0.07951 ± 24	0.6254 ± 22	0.05705 ± 6	493	493	493
M2 small, clear, not abraded	0.036	8.564	5130	1103.9	46	20007	2.072	0.07945 ± 28	0.6248 ± 24	0.05703 ± 4	493	493	493
G97-8 (Ordenes Series migmatite)													
M1 yellow, not abraded	0.024	7.985	3181	984.7	29	12656	3.557	0.07744 ± 22	0.6065 ± 20	0.0568 ± 6	481	481	484

[a] Corrected for fractionation, spike, laboratory blank (2 to 12 pg common lead; 1 pg uranium), and initial common lead from the model of Stacey and Kramers [32].

3.3. Results

The U–Pb results are shown in Table 1. The sample from the Monte Castelo Gabbro (G97-1) yielded abundant fragments of coarse zircon prisms (0.3 mm mean size), very clear, with rare distinguishable crystal faces and edges (Fig. 5b,c). The homogeneity of grain size and morphology of the zircon grains suggest the presence of one single igneous population. Three analyses carried out on mineral fractions with different degrees of abrasion are concordant and overlap, giving a precise age of 499 ± 2 Ma (Fig. 3a), which is interpreted as the age of igneous crystallisation.

The zircons from G97-2, the granitoid rock at the northern contact of MCG, are euhedral elongated prisms ranging in size from 0.1 to 0.5 mm (Fig. 5a). They are clear, with sharp edges and faces and without overgrown rims. Two abraded fractions containing small and large crystals (Z1 and Z2, respectively), gave an almost concordant age of 500 ± 2 Ma (0.9–1% discordant) (Fig. 3b). The granitoid also contains monazites, which are rounded, pale yellow and rather turbid. Some monazites from this and the following samples have an orange surface coating, probably of apatite [33], which was completely removed by air abrasion or HNO_3 cleaning. The two analysed fractions are not duplicated, and plot slightly above the concordia, defining a reverse discordance (Fig. 3b). Fraction M2, formed by the coarse monazite grains (~0.15 mm) provides $^{206}Pb/^{238}U$ and $^{207}Pb/^{235}U$ ages of 498 and 496 Ma,

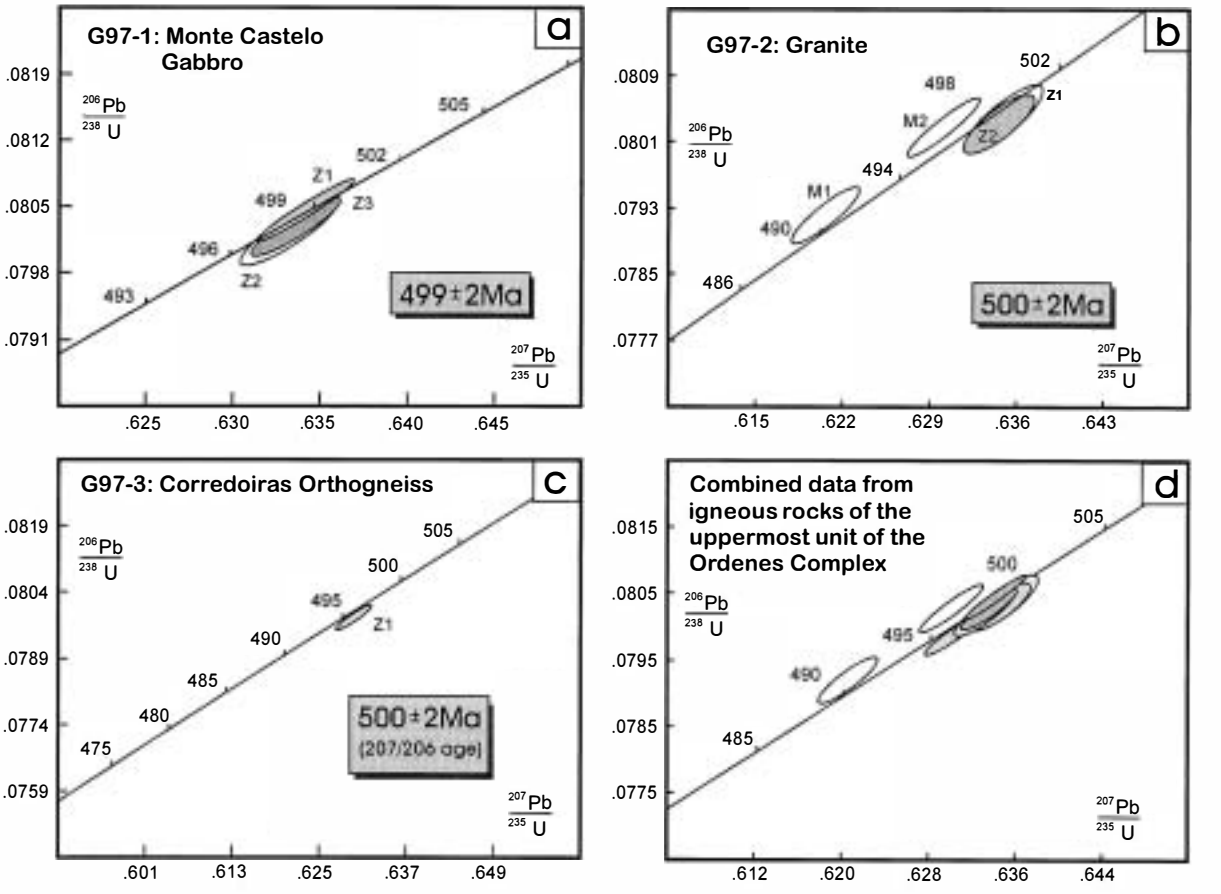

Fig. 3. U–Pb concordia diagrams for the igneous samples from the uppermost unit of the Ordenes Complex. (a) Monte Castelo Gabbro (zircon). (b) Granite located at the north limit of Monte Castelo Gabbro (zircon and monazite). (c) Corredoiras Orthogneiss (zircon). (d) combined data.

respectively, which corroborates the data from the zircon, whereas M1, formed by the small grains (0.05–0.1 mm), gives younger ages ($^{206}Pb/^{238}U$ = 491 Ma; $^{207}Pb/^{235}U$ = 490 Ma). The age difference of the monazite can be attributed to two factors: (1) the smaller grain size of minerals of M1 fraction could favour a lower closing temperature of the U–Pb system; or (2) Pb loss after crystallisation. In the cases of reverse discordance in these analyses, the $^{207}Pb/^{235}U$ age is considered the best estimate of crystallisation of the mineral, although considering the mean of the three apparent U–Pb ages does not modify significantly this age.

One fraction of euhedral, clear zircon prisms from Corredoiras Orthogneiss (G97-3) gives a slightly discordant analysis with a $^{207}Pb/^{206}Pb$ age of 500 ± 2 Ma, very similar to the previous ones (Fig. 3c).

Monazite from the metapelitic granulite G97-4 is euhedral, pale yellow and clear (Fig. 5d,e), and forms a homogeneous population with a mean size of 0.15 mm. Two almost concordant fractions give a $^{207}Pb/^{235}U$ age of 498 ± 2 Ma (duplicated analyses, Fig. 4a) with $^{207}Pb/^{206}Pb$ ages slightly lower (494 and 493 Ma), defining a reverse discordance (−0.9% discordant). Two reddish brown rutile fractions do not yield precise ages due to the large common Pb correction and because the low U and radiogenic Pb contents (5 ppm U; 0.4 ppm radiogenic Pb) increase the uncertainties of the measured isotopic ratios. The $^{206}Pb/^{238}U$ ratio is the most precise and less affected by the common Pb correction, and $^{206}Pb/^{238}U$ ages are probably the best estimates of the closing of the U–Pb system in these rutiles. $^{206}Pb/^{238}U$ ages of 391 ± 3 and 382 ± 3 Ma are about 100 Ma younger than the ages yielded by the monazites in the same sample.

Monazite from the two paragneisses G97-5 and G97-6, from the sillimanite zone, yield similar ages: a concordant age of 496 ± 3 for G97-5 (Fig. 4b), and an age of 493 ± 1 Ma given by a regression line with the lower intercept pinned at 10 ± 10 Ma (G97-6; Fig. 4c). Monazite grains from the former are very tiny (0.02–0.05 mm), lentil-shaped, yellow and turbid (Fig. 5f), whereas monazites from G97-6 are very sparse high-quality grains, subrounded, clear and of 0.1 mm mean size.

The migmatites included in Corredoiras Orthogneiss (G97-7 and G97-8) contain monazites very similar to those of G97-5, and G97-7 also yielded a concordant age of 493 ± 3 (Fig. 4d), whereas G97-8 seems to be slightly younger with a $^{207}Pb/^{206}Pb$ age of 484 ± 2 Ma (Fig. 4e). This last age is less reliable because only one single analysis is available, and it only can be considered as a minimum age.

3.4. Discussion

3.4.1. Age of magmatism

The absence of any inherited component, the very limited Pb loss, and the igneous morphology of zircons, indicate that the obtained ages are the ages of crystallisation of the magmatic bodies. The possibility of some resetting of the U–Pb system during the granulitic metamorphic event subsequent to the crystallisation of the magmas (see above) can be ruled out for several reasons: (1) the characteristic igneous morphology of the zircons without showing any evidence of overgrowths or recrystallisation; (2) the concordant character of the ages suggests that the U–Pb system behaved as a closed system (metamorphosed zircon is generally highly discordant, unless newly crystallised) [34]; (3) Pb diffusion in pristine zircon is insignificant until temperatures above 1000°C [34]; and (4) the literature reports several examples of igneous rocks that have undergone a granulitic metamorphism and the U–Pb system of the zircon remained unaltered [35,36].

3.4.2. Ages of metamorphism

The relatively high closing temperature of monazite, above 700–725°C [8–10], and the general lack of inherited components, makes this mineral specially suitable for dating high-grade thermal events. The growth of monazite during amphibolite- and granulite-facies prograde metamorphism of metasedimentary aluminous rocks is widely documented [9,33,37], and their U–Pb crystallisation ages are frequently interpreted as close to the thermal peak [37–40]. All the ages obtained in this study from upper amphibolite- and granulite-facies metapelites are remarkably uniform and constrained in a narrow interval between 493 and 498 Ma (except G97-8 at 484 Ma). Most of the monazites are found included in biotite lepidoblasts and, therefore, their ages are considered as the maximum ages for the development of the gneissic fabric, probably very

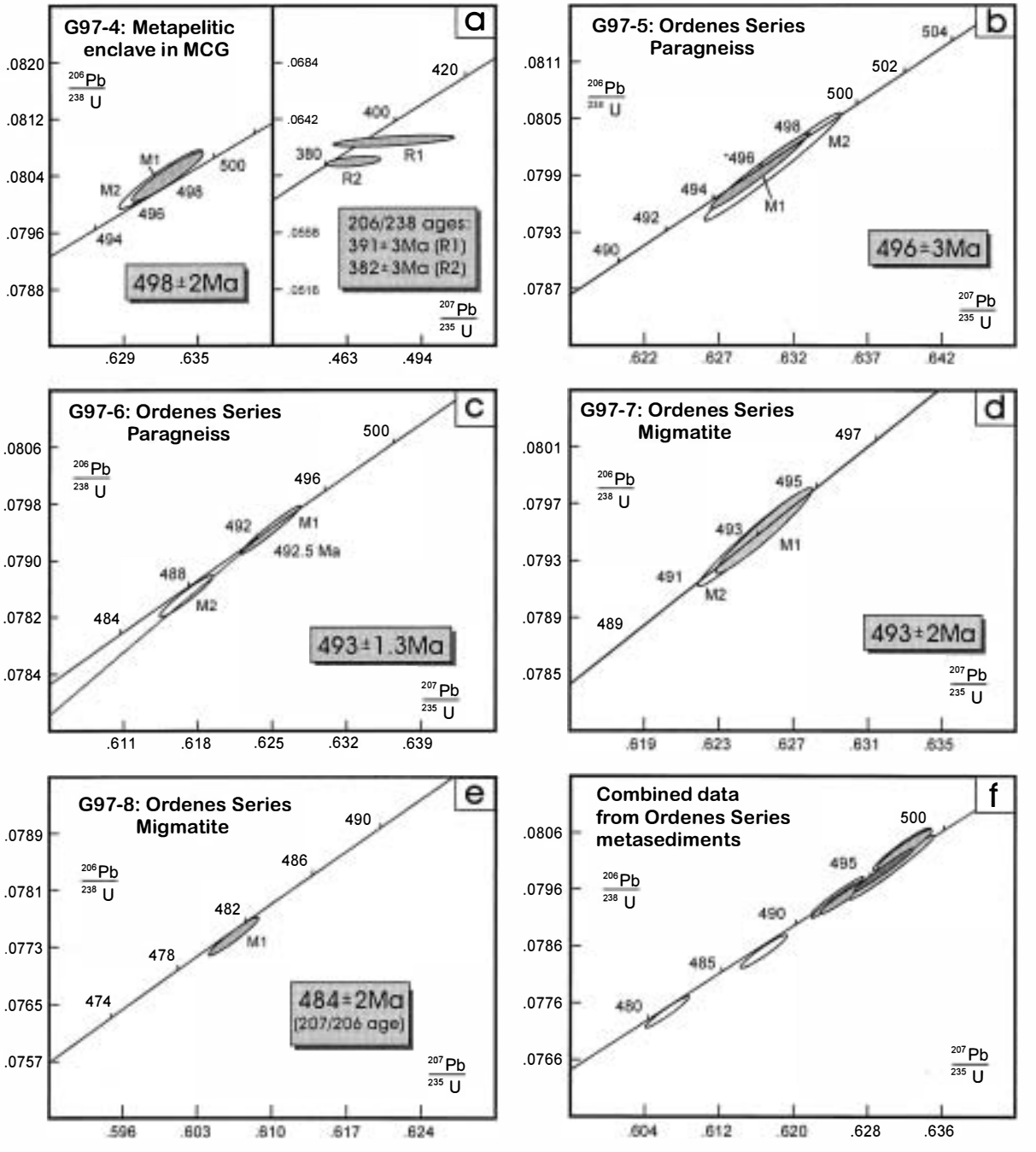

Fig. 4. U–Pb concordia diagrams for the metasedimentary gneisses from the uppermost unit of the Ordenes Complex. (a) Metapelitic enclave in Monte Castelo Gabbro (monazite and rutile). (b) Ordenes Series paragneiss (monazite). (c) Ordenes Series paragneiss (monazite). (d) Ordenes Series migmatite included in Coredoiras Orthogneiss (monazite). (e) Ordenes Series migmatite included in Coredoiras Orthogneiss (monazite). (f) Combined data.

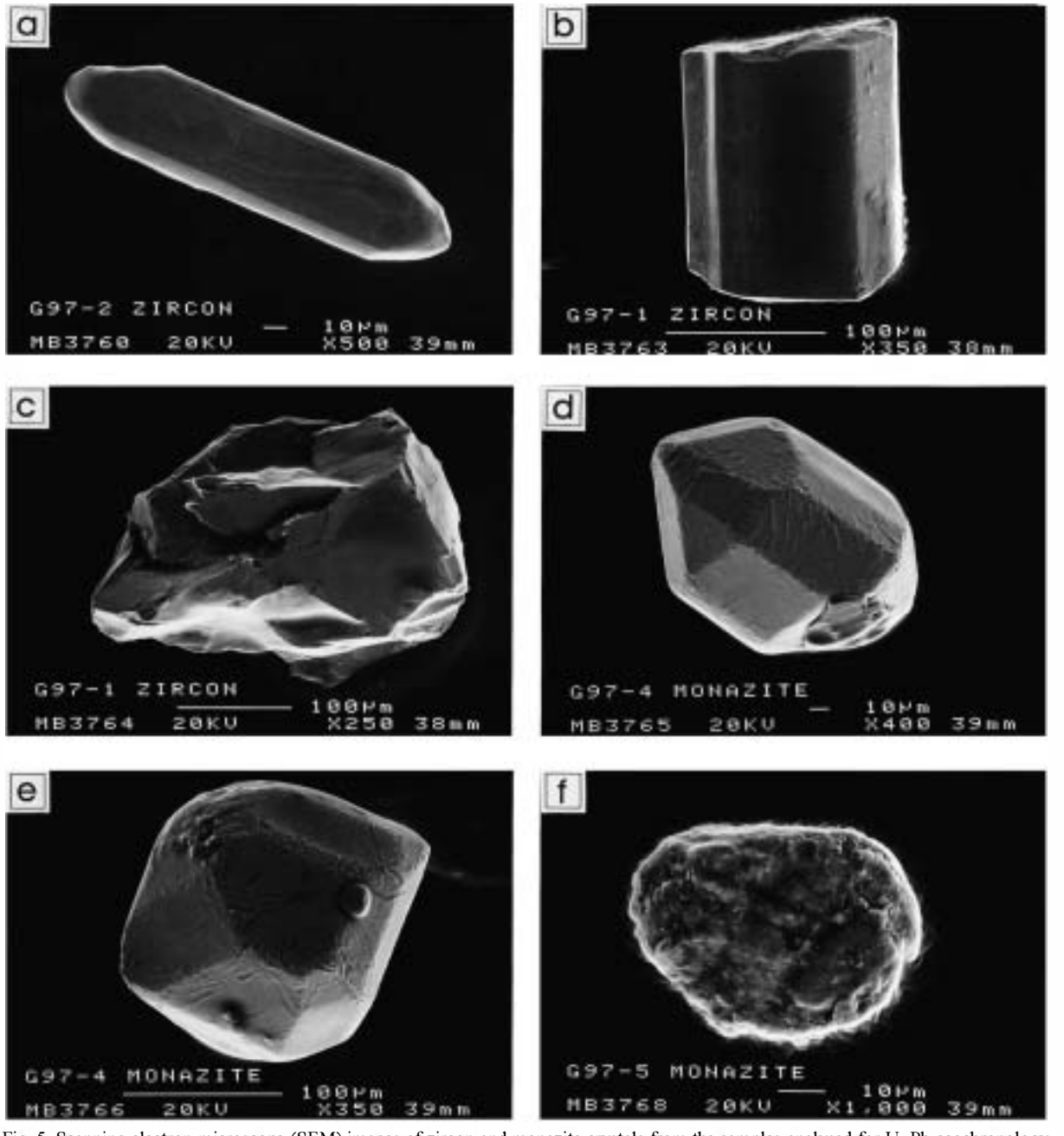

Fig. 5. Scanning electron microscope (SEM) images of zircon and monazite crystals from the samples analysed for U–Pb geochronology. (a) Euhedral zircon prism from granite G97-2. (b) Fragmented zircon prism from Monte Castelo Gabbro (G97-1). (c) Typical irregular morphology (fragmented) of zircon from Monte Castelo Gabbro (G97-1). (d, e) Examples of euhedral monazite from the metapelitic granulite G97-4. (f) Lentil-shape monazite from paragneiss G97-5.

close to the metamorphic peak. Monazite ages of metasediments are only slightly younger than the magmatic zircon ages and both can be considered almost synchronous. This fact can be interpreted in two ways.

(1) Monazites from metasediments could have

been formed by the thermal influence (contact metamorphism) of the plutonic bodies during their intrusion. Then, their ages would be dating magmatism, not metamorphism, and the younger ages of monazites could be explained by a lower closing temperature with respect to zircons. Monazites would be then contact-metamorphism relicts that were overgrown by the biotite lepidoblasts during a later regional metamorphism.

(2) Monazites could reflect a metamorphic event immediately following the intrusion of the igneous bodies.

The former possibility has been ruled out for several reasons.

(1) The metasedimentary rocks were collected over a wide area of the uppermost IP unit, and in some cases (e.g. samples G97-5 and G97-6) far away from the Ordovician plutons (Fig. 2). It seems unlikely that contact metamorphism affected all the sedimentary series, including zones distant from the intrusions.

(2) The metamorphism subsequent to the intrusion of the igneous bodies reaches the granulite facies in the deepest parts of the IP uppermost unit. This fact can be observed for example in the MCG, which is deformed by granulite-facies shear zones (see Section 2.3.2). The temperature conditions typical of the granulite facies are clearly above the closing temperature of the U–Pb system in monazites [8–10], and in consequence a metamorphism with these characteristics should lead to the total resetting, or at least a partial resetting of the system. Therefore, the age of the high-grade metamorphism cannot be later than the age of the monazites.

The previous arguments support the existence of a high-grade metamorphic event immediately following the intrusion of the igneous bodies. The rutile ages of 380–390 Ma imply a great time span from the high-grade event if they were interpreted as cooling ages. The closure temperature of the U–Pb system in rutile is estimated around 450°C [41] leading to an unrealistically slow cooling rate. Therefore, we interpret this age as a new thermal event between 450° and 650°C, probably related to the accretion and stacking of the uppermost unit to the Variscan orogenic wedge [4].

4. Significance of the new ages in the interpretation of the upper units

The U–Pb isotopic ages of the Monte Castelo Gabbro, the granitoid rocks and the high-grade metasedimentary rocks, clustering between 493 and 500 Ma, indicate that emplacement of the igneous bodies was immediately followed by their burial and by a regional Barrovian-type metamorphism that reached granulite facies. Furthermore, we must keep in mind that the chemistry of the MCG points to a volcanic arc setting, but also that the chemistry of the gabbros of the HP–HT units [22,23], point to an intracontinental extensional regime of roughly the same age [5].

A convergent scenario seems to fit the different data. We suggest that the uppermost IP unit represents an accretionary complex, built with sediments deposited adjacent to a volcanic arc or in a previously passive continental margin. The gabbros resulted from the subduction of the oceanic lithosphere, whereas the granitoids developed by partial melting of the thickened wedge, and were themselves, together with the gabbros, buried and metamorphosed shortly after their emplacement. The extensional regime indicated by the chemistry of the gabbros of the HP–HT units [22,23], may reflect the separation of the volcanic arc from the continental realm where it was initially developed. The MORB-type REE pattern of eclogites [21] in the HP–HT units may indicate that oceanic lithosphere was generated in a back-arc setting.

This Early Ordovician plate convergence poses a problem in the context of Gondwana–Laurentia interactions. It is true that the new plutonic and metamorphic ages correlate with the Taconic event in the Appalachians and contemporaneous events (Finnmarkian, Grampian) in other parts of the Caledonian belt. But these episodes are commonly ascribed to convergence within the Iapetus ocean, and occurred along the northern side of Avalon [12,42]. By that time, the northern margin of Gondwana was apparently undergoing extension, leading to the separation of Avalon and the opening of the Rheic ocean [11,12]. Avalon is the outermost emergent terrane in the margin of the North Atlantic Ocean opposite to the Iberian Peninsula, and was adjacent or very close to western Iberia before the break up

of Pangea (Fig. 1). Characterised by its Gondwanan provenance and Pan-African deformation and magmatism ([43], and references therein), no Ordovician orogenic events have been reported for Avalon.

A possible explanation is that oblique movements between Laurentia and Gondwana, and/or a complex scenario involving several microcontinents, could have inserted an exotic volcanic arc or a convergent plate margin in the Rheic ocean, between Gondwana and Avalon [44]. However, the development of an Ordovician convergent margin and associated magmatism within Gondwana itself has been documented at least for the central Andes in Argentina [45], and Early Ordovician metamorphic ages have been found in the Variscan basement of central Europe and the Alps, also in relation with the margin of Gondwana [46]. Furthermore, Sandeman et al. [47] have found rocks of volcanic-arc affinity and similar protolith age (499^{+8}_{-3} Ma) adjacent to the Lizard ophiolite, in the Variscan belt of SW England. Consequently, the possibility that the orogenic episode identified in the uppermost units of the Iberian allochthon could have occurred in either the Gondwana or Rheic domains cannot be ruled out.

Martínez Catalán et al. [4] put forward an accretionary model for the Iberian allochthonous complexes. According to this model, the continental margin of Laurentia registered, after the early amalgamations of volcanic arcs related to the Taconic event, the successive incorporation of Avalon, pieces of the Rheic oceanic lithosphere, and the collision of the outermost margin of Gondwana. Now, we should add an accretionary complex, probably related to an Early Ordovician island arc, which subsequently became involved in the Variscan convergence and accretion. An updated version of the Variscan accretionary history can be seen in Martínez Catalán et al. [48]. However, a version including the position and polarity of subduction of the former Early Ordovician accretionary complex cannot be drawn yet, due to the lack of reliable data.

The Iberian allochthonous units were accreted during the Early and Middle Devonian [2,4,20,24]. The 390–380 Ma ages obtained from two rutile fractions of the metapelitic granulite included in Monte Castelo Gabbro, may reflect cooling following the first Variscan tectonothermal event in the uppermost unit. The HP–HT upper units registered an Early Devonian metamorphic episode, between 405 and 390 m.y. ago [5–7]. It is not clear if these ages correspond to the high-pressure and high-temperature event or not. Our discovery of a Lower Ordovician Barrovian metamorphism in the IP uppermost unit suggests that an older age is also possible for the HP–HT event, as was proposed by Kuijper [26] and Peucat et al. [21]. In any case, we suggest that the 405–390 Ma ages reflect the accretion of the upper units to the wedge under development at the southern margin of Avalon. Their deformation and metamorphism would be related either to subduction, if the HP event is Early Devonian, or to underthrusting and crustal thickening, if it is Early Ordovician.

5. Conclusions

An Early Ordovician magmatic and metamorphic event, constrained between 493 and 500 Ma, has been identified by U–Pb geochronology in the uppermost unit of the Ordenes Complex, in NW Spain. The Barrovian character of the metamorphism clearly points to crustal thickening and, consequently, reveals a compressional tectonic event. Taking into account the chemical signature of the gabbros and the flyschoid character of the metasediments, the uppermost units of the allochthonous complexes in the Iberian Peninsula, occurring above the ophiolites marking the suture, are considered pieces of an Early Ordovician accretionary complex. This implies a relationship with a convergent plate margin, and suggests a volcanic arc as the more probable setting for these uppermost units. The underlying HP–HT upper units, also in the hangingwall to the suture, may be related to the same volcanic arc, and former interpretations of Early Ordovician isotopic data as metamorphic ages should be considered again, in the light of the new results from the uppermost unit of the Ordenes Complex.

Convergent plate boundaries seem to have existed in other marginal areas of Gondwana during the Ordovician and, in particular, have been identified in the Variscan basement of central Europe and the Alps. In spite of the dominantly extensional regime that is often assumed for this period in the NE margin of the Paleozoic supercontinent (opening of the Rheic ocean), very little is known of the de-

tailed plate configuration and kinematics of the Rheic ocean and the Avalon microcontinent(s). In this context, our data support the existence of short-lived convergent plate boundaries in the realm between Laurentia and Gondwana during the early Paleozoic, but more data will be necessary to constrain their extent, geometry and polarity of subduction.

Acknowledgements

We are grateful to K. Brueckner, Ph. Matte and K. Mezger for critical review of the manuscript that helped us to improve its quality. Support for this work was provided by grants PB94-1396-C02 and APC1997-0011 of the Spanish DGICYT. *[CL]*

References

[1] A. Ribeiro, E. Pereira, R. Dias, Central-Iberian Zone, Allochthonous sequences, Structure in the northwest of the Iberian Peninsula, in: R.D. Dallmeyer, E. Martinez García (Eds.), Pre-Mesozoic Geology of Iberia, Springer, Berlin, 1990, pp. 220–236.

[2] J.R. Martínez Catalán, R. Arenas, F. Díaz García, F.J. Rubio Pascual, J. Abati, J. Marquínez, Variscan exhumation of a subducted Paleozoic continental margin: the basal units of the Ordenes Complex, Galicia, NW Spain, Tectonics 15 (1996) 106–121.

[3] J. Blaise, E. Bouyx, Les séries cambro-ordoviciennes à Cruziana et le problème de l'extension septentrionale des plate-formes 'perigondwaniennes' durant le Paléozoïque inférieur, C.R. Acad. Sci. Paris 291 (1980) 793–796.

[4] J.R. Martínez Catalán, R. Arenas, F. Díaz García, J. Abati, Variscan accretionary complex of northwest Iberia: terrane correlation and succession of tectonothermal events, Geology 27 (1997) 1103–1106.

[5] H.J. Schäfer, D. Gebauer, J.I. Gil Ibarguchi, J.J. Peucat, Ion-microprobe U–Pb zircon dating on the HP/HT Cabo Ortegal Complex (Galicia, NW Spain): preliminary results, Terra Nova Abstr. Suppl. 4 (1993) 22.

[6] J.F. Santos Zalduegui, U. Schärer, J.I. Gil Ibarguchi, J. Girardeau, Origin and evolution of the Paleozoic Cabo Ortegal ultramafic–mafic complex (NW Spain): U–Pb, Rb–Sr and Pb–Pb isotope data, Chem. Geol. 129 (1996) 281–304.

[7] B. Ordoñez Casado, D. Gebauer, H.J. Schäfer, J.I. Gil Ibarguchi, J.J. Peucat, A single subduction event at ca. 392 Ma for the ultramafic–mafic HP/HT-rocks of the Cabo Ortegal Complex, Geogaceta 20 (1996) 489–490.

[8] P. Copeland, R.R. Parrish, T.M. Harrison, Identification of inherited radiogenic Pb in monazite and implications for U–Pb systematics, Nature 333 (1988) 760–763.

[9] R.R. Parrish, U–Pb dating of monazite and its application to geological problems, Can. J. Earth Sci. 27 (1990) 1431–1450.

[10] K. Mezger, C.M. Rawnsley, S.R. Bohlen, G.N. Hanson, U–Pb garnet, titanite, monazite and rutile ages: implications for the duration of high grade metamorphism and cooling histories, Adirondack Mountains, New York, J. Geol. 99 (1991) 415–428.

[11] R.A. Fortey, L.R.M. Cocks, Arenig to Llandovery faunal distributions in the Caledonides, in: A.L. Harris, D.J. Fettes (Eds.), The Caledonian–Appalachian Orogen, Geol. Soc. London Spec. Publ. 38 (1988) 233–246.

[12] N.J. Soper, Timing and geometry of collision, terrane accretion and sinistral strike-slip events in the British Caledonides, in: A.L. Harris, D.J. Fettes (Eds.), The Caledonian–Appalachian Orogen, Geol. Soc. London Spec. Publ. 38 (1988) 481–492.

[13] F. Díaz García, La geología del sector occidental del Complejo de Ordenes (Cordillera Hercínica, NW de España), Nova Terra, Ediciones O Castro, 1990, 230 pp.

[14] R. Arenas, F.J. Rubio Pascual, F. Díaz García, J.R. Martínez Catalán, High-pressure micro-inclusions and development of an inverted metamorphic gradient in the Santiago Schists (Ordenes Complex, NW Iberian Massif, Spain): evidence of subduction and syn-collisional decompression, J. Metamorph. Geol. 13 (1995) 141–164.

[15] P.W.C. Van Calsteren, N.A.I.M. Boelrijk, E.H. Hebeda, H.N.A. Priem, E. Den Tex, E.A.T.H. Verdurmen, R.H. Verschure, Isotopic dating of older elements (including the Cabo Ortegal mafic–ultramafic complex) in the Hercynian Orogen of NW Spain: manifestations of a presumed early Paleozoic Mantle-plume, Chem. Geol. 24 (1979) 35–56.

[16] J.F. Santos Zalduegui, U. Schärer, J.I. Gil Ibarguchi, Isotope constraints on the age and origin of magmatism and metamorphism in the Malpica–Tuy allochthon, Galicia, NW-Spain, Chem. Geol. 121 (1995) 91–103.

[17] M.L. Ribeiro, P. Floor, Magmatismo peralcalino no Maciço Hespérico: sua distribução e significado geodinámico, in: F. Bea, A. Carnicero, J.C. Gonzalo, M. López-Plaza, M.D. Rodríguez Alonso (Eds.), Geología de los granitoides y rocas asociadas del Macizo Hespérico, Rueda, Madrid, 1987, pp. 211–221.

[18] R. Arenas, J. Abati, J.R. Martínez Catalán, F. Díaz García, F.J. Rubio Pascual, P–T evolution of eclogites from the Agualada Unit (Ordenes Complex, NW Iberian Massif, Spain): implications for crustal subduction, Lithos 40 (1997) 221–242.

[19] G.R. Dunning, F. Díaz García, R. Arenas, J.R. Martínez Catalán, A Lower Devonian Ophiolite in the Allochthonous Complexes of the Iberian Massif (Variscan Belt): U–Pb zircon protolith age from the Careón ophiolite, Terra Abstr. 9 (1) (1997) 100.

[20] R.D. Dallmeyer, A. Ribeiro, F. Marques, Polyphase Variscan emplacement of exotic terranes (Morais and Bragança Massifs) onto Iberian successions: evidence from $^{40}Ar/^{39}Ar$ mineral ages, Lithos 27 (1991) 133–144.

[21] J.J. Peucat, J. Bernard-Griffiths, J.I. Gil Ibarguchi, R.D. Dalhneyer, R.P. Menot, J. Cornichet, M. Iglesias Ponce de

León, Geochemical and geochronological cross section of the deep Variscan crust: the Cabo Ortegal high-pressure nappe (northwestern Spain), Tectonophysics 177 (1990) 263–292.
[22] P.W.C. Van Calsteren, E. Den Tex, An early Paleozoic continental rift system in Galicia (Spain), in: I.B. Ramberg, E.R. Neumann (Eds.), Tectonics and Geophysics of Continental Rifts, Reidel, Dordrecht, 1978, pp. 25–132.
[23] G. Galán, A. Marcos, Geochemical evolution of high-pressure mafic granulites from the Bacariza formation (Cabo Ortegal complex, NW Spain): an example of a heterogeneous lower crust, Geol. Rundsch. 86 (1997) 539–555.
[24] R.D. Dalhneyer, J.R. Martínez Catalán, R. Arenas, J.I. Gil Ibarguchi, G. Gutierrez Alonso, P. Farias, F. Bastida, J. Aller, Diachronous Variscan tectonothermal activity in the NW Iberian Massif: evidence from $^{40}Ar/^{39}Ar$ dating of regional fabrics, Tectonophysics 227 (1997) 307–337.
[25] P. Matte, R. Capdevila, Tectonique en grands plis couchés et plissements superposés d'âge hercynien dans la série de Ordenes-Betanzos (Galice Occidentale), Cuad. Seminar. Estud. Cerámicos Sargadelos 27 (1978) 193–201.
[26] R.P. Kuijper, U–Pb systematics and the petrogenetic evolution of infracrustal rocks in the Paleozoic basement of Western Galicia, NW Spain, Verh. ZWO Lab. Isot. Geol. Amsterdam 5 (1979) 1–101.
[27] R.D. Dallmeyer, R.D. Tucker, U–Pb zircon age for the Lagoa augengneiss, Morais Complex, Portugal: tectonic implications, J. Geol. Soc. London 150 (1993) 405–410.
[28] B. Dubé, G.R. Dunning, K. Lauzière, J.C. Roddick, New insights into the Appalachian Orogen from geology and geochronology along the Cape Ray fault zone, southwest Newfoundland, Geol. Soc. Am. Bull. 108 (1996) 101–116.
[29] T.E. Krogh, Improved accuracy of U–Pb zircon ages by the creation of more concordant systems using air abrasion technique, Geochim. Cosmochim. Acta 46 (1982) 637–649.
[30] T.E. Krogh, A low contamination method for hydrothermal decomposition of zircon and extraction of U and Pb for isotopic age determination, Geochim. Cosmochim. Acta 37 (1973) 485–494.
[31] G. Manhès, J.F. Minster, C.J. Allègre, Comparative uranium–thorium–lead and rubidium–strontium study of the Saint Séverin amphoterite: consequence for early solar system chronology, Earth Planet. Sci. Lett. 39 (1978) 14–24.
[32] J.S. Stacey, J.D. Kramers, Approximation of terrestrial lead isotope evolution by a two-stage model, Earth Planet. Sci. Lett. 26 (1975) 207–221.
[33] A. Lanzirotti, G.N. Hanson, Geochronology and geochemistry of multiple generations of monazite from the Wepawaug Schist, Connecticut, USA: implications for monazite stability in metamorphic rocks, Contrib. Mineral. Petrol. 125 (1996) 332–340.
[34] K. Mezger, E.J. Krogstad, Interpretation of discordant U–Pb zircon ages: an evaluation, J. Metamorph. Geol. 15 (1997) 127–140.
[35] J.R. Chiarenzelli, J.M. McLelland, Granulite facies metamorphism, palaeoisotherms and disturbance of the U–Pb systematics of zircon in anorogenic plutonic rocks from the Adirondack Highlands, J. Metamorph. Geol. 11 (1993) 59–70.
[36] S. Hölzl, A.W. Hofmann, W. Todt, H. Köhler, U–Pb geochronology of the Sri Lanka basement, Precambrian Res. (1994) 123–149.
[37] H.A. Smith, B. Barreiro, Monazite U–Pb dating of staurolite grade metamorphism in pelitic schists, Contrib. Mineral. Petrol. 105 (1990) 602–615.
[38] J.D. Eusden, B. Barreiro, The timing of peak high-grade metamorphism in central-eastern New England, Marit. Sediments Atlantic Geol. 24 (1988) 241–255.
[39] F. Childe, R. Doig, C. Gariépy, Monazite as a metamorphic chronometer, south of the Grenville Front, western Quebec, Can. J. Earth Sci. 30 (1993) 1056–1065.
[40] P.A. Cawood, G.R. Dunning, D. Lux, J.A.M. van Gool, Timing of peak metamorphism and deformation along the Appalachian margin of Laurentia in Newfoundland: Silurian, not Ordovician, Geology 22 (1994) 399–402.
[41] K. Mezger, G.N. Hanson, S.R. Bohlen, High-precision U–Pb ages of metamorphic rutile: application to the cooling history of high grade terranes, Earth Planet. Sci. Lett. 96 (1989) 106–118.
[42] R.B. Neuman, M.D. Max, Penobscottian–Grampian–Finnmarkian orogenies as indicators of terrane linkages, in: R.D. Dalhneyer (Ed.), Terranes in the Circum-Atlantic Paleozoic Orogens, Geol. Soc. Am. Spec. Pap. 230 (1989) 31–45.
[43] J.V. Skehan, N. Rast, Late Proterozoic to Cambrian evolution of the Boston Avalon Terrane, in: J.P. Hibbard, C.R. Van Staal, P.A. Cawood (Eds.), Current Perspectives in the Appalachian–Caledonian Orogen, Geol. Assoc. Can. Spec. Pap. 41 (1995) 207–225.
[44] J.R. Martínez Catalán, A non-cylindrical model for the northwest Iberian allochthonous terranes and their equivalents in the Hercynian belt of Western Europe, Tectonophysics 179 (1990) 253–272.
[45] V. Ramos, The tectonics of the Central Andes; 30° to 33°S latitude, in: S.P. Clark, B.C. Burchfiel, J. Suppe (Eds.), Processes in Continental Lithospheric Deformation, Geol. Soc. Am. Spec. Pap. 218 (1988) 31–54.
[46] J.F. Von Raumer, F. Neubauer, Late Precambrian and Paleozoic evolution of the Alpine basement — an overview, in: J.F. Von Raumer, F. Neubauer (Eds.), Pre-Mesozoic Geology in the Alps, Springer, Berlin, 1993, pp. 625–639.
[47] H.A. Sanderman, A.H. Clark, M.T. Styles, D.J. Scott, J.G. Malpas, E. Farrar, Geochemistry and U–Pb and $^{40}Ar–^{39}Ar$ geochronology of the Man of War Gneiss, Lizard Complex, SW England: pre-Hercynian arc-type crust with a Sudeten–Iberian connection, J. Geol. Soc. London 154 (1997) 403–417.
[48] J.R. Martínez Catalán, R. Arenas, F. Díaz García, J. Abati, Allochthonous units in the Variscan belt of NW Iberia. Terranes and accretionary history, in: A.K. Sinha (Ed.), Basement Tectonics 13; Proceedings of the Thirteenth International Conference on Basement Tectonics, Blacksburg, VA, June 1997 (in press).
[49] J.P. Lefort, Basement Correlation across the North Atlantic, Springer, Berlin, 1989, 148 pp.